Appl. Phys. B 81, 277–281 (2005)
DOI: 10.1007/s00340-005-1858-6

Applied Physics B
Lasers and Optics

M. BOTEY[1]
M. MAYMÓ[2,3]
J. MARTORELL[2,3,✉]

Band-structure determination for finite 3-D photonic crystals

[1]Departament de Física i Enginyeria Nuclear, Universitat Politècnica de Catalunya, Comte d'Urgell 187, 08036 Barcelona, Spain
[2]Departament de Física i Enginyeria Nuclear, Universitat Politècnica de Catalunya, Colom 11, 08222 Terrassa, Spain
[3]ICFO – Institut de Ciències Fotòniques, Jordi Girona 29, Nexus II, 08034 Barcelona, Spain

Received: 2 February 2005
Published online: 15 July 2005 •

ABSTRACT The partial band structure from a finite photonic crystal is determined using a model based on light diffraction and the transfer-matrix formalism. The predictions from such a model are compared to an experimental measurement of the bands in the LU direction of a face centered cubic colloidal crystal. Then, both the theoretical predictions and the experimental measurements are compared with the usual band-structure calculation based on a plane-wave expansion with perfectly periodic boundary conditions. As in measurements performed in the past, discrepancies between the predictions of this later model and the experimentally determined bands are observed. On the contrary, using the model presented based on light propagation through a finite crystal, where no periodicity is imposed in the direction perpendicular to any of the set of planes considered to determine a specific branch of the band structure, we found a very good agreement between the experimentally determined and the predicted bandwidths.

PACS 42.70.Qs; 42.25.Fx

1 Introduction

Since 1987 when Eli Yablonovitch [1] proposed that three-dimensional (3-D) periodic arrays of dielectric material could be used to achieve a full inhibition of the spontaneous emission, there have been numerous studies, theoretical and experimental, that considered light propagation in a large variety of 3-D periodically microstructured materials; see e.g. [2, 3]. In such studies, a major step forward was achieved when a full wave-vector analysis was used to predict the band structure of 3-D photonic crystals, which at that time were referred to solely as photonic band gap materials [4–6]. However, already in the early days of the photonic crystal field, a disagreement between experimental results and some of the predictions of the band-structure numerical determination, based on a plane-wave expansion with periodic boundary conditions, was reported. Tarhan and Watson [7] pointed out that the predicted degeneracy at the W point of the first Brillouin zone (FBZ) of a face centered cubic (fcc) crystal was not seen experimentally. More recently, very accurate experimental measurements of the LU bands of an artificial opal made of silica spheres [8] showed a clear deviation at large angles with respect to the numerical prediction of band diagrams based on a plane wave expansion calculation. A more consistent discrepancy has been found between the theoretical predictions of the spontaneous emission factor and the several experimental measurements of that factor in photonic crystals with a pseudo-gap that have been reported since Yablonovitch's proposal [9–12].

In a recent work it was pointed out that the finiteness of real photonic crystals may play an important role in the changes induced in phenomena such as the inhibition of spontaneous emission. In that work, Felbacq and Smaâli [13] noted that the strong interaction of photons with the boundary of a photonic structure gives rise to a difficulty in establishing a rigorous link between finite and infinite structures with perfectly periodic boundary conditions. In the present paper, we present an alternative route to determine the bands of a 3-D photonic crystal without imposing any periodic boundary conditions in the direction perpendicular to any one of the set of planes we will consider to determine a specific branch of that band structure. The predictions of our model are then compared with an experimental measurement of the s and p polarization LU bands of a face centered cubic (fcc) structure for a photonic crystal fabricated from a colloidal suspension of highly monodisperse microspheres. Finally, both results are compared with a determination of the same bands following the usual plane-wave approximation with periodic boundary conditions in the three space directions.

2 Wave propagation in 3-D photonic crystals

A partial calculation of the band diagrams of a finite crystal is possible if one considers wave propagation with respect to each set of planes separately. To consider full wave vector propagation with respect to a given set of planes of the lattice, we extend the model developed in Ref. [14] to include both, the transversal, as well as, the longitudinal components

✉ Fax: +34-93-739-8101, E-mail: jordi.martorell@upc.edu

of the electromagnetic field. This is done by writing a wave equation for the vector potential $\mathbf{A}$ in the gauge where $\nabla\mathbf{A} = \mathrm{i}\omega\varepsilon(\boldsymbol{r})\mu_0\Phi$ (Φ is a scalar potential function). In the present case, as opposed to the treatment in Ref. [14], zero divergence of the electric field is not assumed. Under the assumption of harmonic solutions, the wave equation for the vector potential at frequency ω takes the form

$$\nabla^2\mathbf{A} + \omega^2\varepsilon(\boldsymbol{r})\,\mu_0\mathbf{A} = -\mu_0\mathbf{J}. \tag{1}$$

Then, we express the vector potential and the electric fields both as a superposition of plane waves: $\mathbf{E} = \int \mathrm{d}^3\mathbf{k}\ \mathbf{E}_\mathrm{k}\mathrm{e}^{\mathbf{ikr}}$, $\mathbf{A} = \int \mathrm{d}^3\mathbf{k}\ \mathbf{A}_\mathrm{k}\mathrm{e}^{\mathbf{ikr}}$; and expand the dielectric constant as a Fourier series on the xy plane:

$$\frac{\varepsilon(\mathbf{r})}{\varepsilon_0} - 1 = \sum_{\mathbf{G}_\mathrm{mn}} \varepsilon_{\mathbf{G}_\mathrm{mn}}(z)\mathrm{e}^{\mathbf{i}\mathbf{G}_\mathrm{mn}\mathbf{r}}, \tag{2}$$

where $\mathbf{G}_\mathrm{mn} = m\mathbf{b}_1 + n\mathbf{b}_2$, and $\mathbf{b}_1$ and $\mathbf{b}_2$ are the unit reciprocal-lattice vectors lying on one of the planes of the set we are considering which is parallel to the xy plane.

After substitution of the expansions of the electric field, vector potential, and dielectric constant into Eq. (1), we obtain

$$\left(\frac{\mathrm{d}^2}{\mathrm{d}z^2} + k_z^2\right)\mathbf{A}_{\mathbf{k}_\rho}(z) = \frac{\mathrm{i}\omega n_\mathrm{w}^2}{c^2}\sum_{\mathbf{G}_\mathrm{mn}} \varepsilon_{\mathbf{G}_\mathrm{mn}}(z)\mathbf{E}_{\mathbf{k}_\rho-\mathbf{G}_\mathrm{mn}}(z), \tag{3}$$

where n_w is the index of the surrounding medium, z is taken perpendicular to the plane set, and $\mathbf{k}_\rho$ is the component of the wave vector perpendicular to the z direction. Because all planes of the set, even the first and last, are surrounded by the same medium, we may solve Eq. (3) for a single plane, determine the electric and magnetic field amplitudes from $\mathbf{A}(\mathbf{r})$. Note that this type of solution will retain all the essential features of a 3-D lattice without the need to impose periodic boundary conditions in the direction perpendicular to that plane set. As in Ref. [14], one may solve Eq. (3) with the use of Green-function integration and obtain an analytical expression for the reflected wave vector potential:

$$\mathbf{A}_{\mathrm{k}_\rho}(z) = \frac{\omega}{2k_z}\mathrm{e}^{-\mathrm{i}k_z z}\int_{-\infty}^{+\infty}\sum_{\mathbf{G}_\mathrm{mn}} \varepsilon_{\mathbf{G}_\mathrm{mn}}(z')\mathbf{E}_{\mathbf{k}_\rho-\mathbf{G}_\mathrm{mn}}(z')\mathrm{e}^{\mathrm{i}k_z z}\mathrm{d}z'. \tag{4}$$

Integration of the right-hand side of Eq. (4) requires knowledge of the electric field within each one of the spheres and the relative amplitudes between each one of the $\mathbf{E}_{k\rho}$ modes of the expansion. Such relative field amplitudes for the s and p polarization may be obtained after solving the $3N\times 3N$-order (N is the number of reciprocal-lattice vectors in the xy plane considered in the summation) determinant of the nontrivial solution of the linear equations for the electric field amplitudes $\mathbf{E}_{\mathrm{k}_z,\mathbf{k}_\rho}$,

$$\mathbf{k}\times\left(\mathbf{k}\times\mathbf{E}_{\mathrm{k}_z,\mathbf{k}_\rho}\right) + \frac{\omega^2}{c^2}\mathbf{E}_{\mathrm{k}_z,\mathbf{k}_\rho} + \frac{\omega^2 n^2}{c^2}\sum_{\mathbf{G}_\mathrm{mn}}\varepsilon_{\mathbf{G}_\mathrm{mn}}\mathbf{E}_{\mathrm{k}_z,\mathbf{k}_\rho-\mathbf{G}_\mathrm{mn}} = 0, \tag{5}$$

which are obtained after converting Maxwell's equations into algebraic ones when using the electric field and dielectric constant expansions given above. In our numerical calculation, summation over $\mathbf{G}_\mathrm{mn}$ is truncated when the convergence error is assured to be below 1%. This procedure is the usual one to determine band structure based on a plane-wave expansion, but applied here only to the in-plane directions.

As pointed out above, the last step before integration of Eq. (4) is to determine the electric field amplitude inside the sphere or, equivalently, the zero-order mode of the expansion appearing in the same equation (4). We apply, then, the Rayleigh–Gans approximation with two additional corrections: the local field correction [15][1] and a modified WKB [16] approximation which corrects the amplitude of the incident wave by introducing the corresponding Fresnel factors[2]. By setting the appropriate boundary conditions for both polarizations, following Ref. [17] we obtain an analytical expression for the s and p polarization reflectivities from a single plane of the set, which in the case of the (111) set take the following form:

$$r_\mathrm{s}(\mathbf{k}) = \mathrm{i}\frac{\pi k^2 D^3}{3\sqrt{3}k_z a^2}(\varepsilon_\mathrm{r}-1)\sum_{\mathrm{G}_\mathrm{mn}} F_\mathrm{mn}\left(\frac{3}{\varepsilon_\mathrm{r}+2}\right)t_\mathrm{s}\left|\mathbf{E}^\mathrm{s}_{k_z\mathbf{k}_\rho-\mathbf{G}_\mathrm{mn}}\right|,$$

$$r_\mathrm{p}(\mathbf{k}) = \mathrm{i}\frac{\pi k^2 D^3}{3\sqrt{3}k_z a^2}(\varepsilon_\mathrm{r}-1)\sum_{\mathrm{G}_\mathrm{mn}} F_\mathrm{mn}\left(\frac{3}{\varepsilon_\mathrm{r}+2}\right)t_\mathrm{p}\left|\mathbf{E}^\mathrm{p}_{k_z\mathbf{k}_\rho-\mathbf{G}_\mathrm{mn}}\right| \tag{6}$$
$$-\mathrm{i}\frac{\boldsymbol{P}_\mathrm{st}}{\epsilon_0 n_\mathrm{w}^2 E_\mathrm{in}}|\mathbf{k}_\rho|,$$

where $\boldsymbol{P}_\mathrm{st}$ is a surface polarization bound to the plane of spheres [17], E_in is the amplitude of the incident field, k is the modulus of the wavevector in the surrounding medium, D is the sphere diameter, a is the separation between spheres on the triangular lattice of the (111) planes, and F_mn are the form factors resulting from the integration over z' in Eq. (4) [14]. Note that the s and p superscripts indicate a different set of amplitudes in each case. Similar expressions can be determined for the (200) direction. Then, using such reflectivity coefficients and applying the transfer-matrix method, one may determine the band in a given direction, let us say for instance the LU direction, from a numerical calculation of the transmission band, which in that case would be affected, essentially, by the reflection coming from the (111) and (200) set of planes.

3 Experimental determination of the LU band

With the appropriate conditions, colloidal particles tend to self-organize in a fcc lattice with the (111) planes parallel to the faces of the container. It is possible to propagate light through the lattice at small angles with respect to the normal to the plane set is possible using different kinds of optical probes. As a result, experimental data to determine for instance the LU, LK, or LW band can be obtained to establish a comparison with the numerical determination of the same band.

[1] Although the local field correction is not commonly used in the Rayleigh–Gans approximation, it improves the accuracy of such approximation, as noted.

[2] We introduce the amplitude transmission Fresnel coefficients, t_s and t_p, for the s and p polarizations, respectively, for a boundary between a first medium with index n_w and a second medium with index $n_\mathrm{avg} = f\,n_\mathrm{sp} + (1-f)n_\mathrm{w}$, where f is the filling fraction of the spheres in the plane.

We performed the experimental measurement of the band using an ordered colloidal suspension of charged monodisperse polystyrene spheres of 147-nm diameter (refractive index $n_{sp} = 1.59$) in water ($n_w = 1.33$). The photonic crystal was grown in a 200-μm-thick precision cell that contained in the bottom a mixed bed ion exchange resin. To tune the position of the Bragg reflection band of the (111) planes, the concentration of the colloidal suspension was accurately controlled before being introduced into the cell. At a high concentration of spheres (8.16×10^{13} spheres/cm^3, a filling fraction of 11.7%) and when stray ions in the water solution diffuse towards the ion-exchange resin, the microspheres self-organize in a fcc lattice. The Bragg condition for the (111) planes at normal incidence is satisfied at a wavelength in vacuum of 576 nm, which corresponds to a lattice constant of 366 nm. To orient the sample, as well as to find a single-crystal domain larger than the transversal dimensions of our probe beam, we illuminated the crystal with a 380-nm laser beam and studied the Kossel line patterns [18–19]. In principle, the only direction known is ΓL, perpendicular to the (111) planes. Therefore, we proceeded as in Ref. [7], illuminating the crystal perpendicular to the cell face and tilting it towards the crossing of 111, $\bar{1}$11, and 200 Kossel lines of the fcc structure. This intersection corresponds to the W point of the fcc FBZ in reciprocal lattice space. We can then determine the U and K points.

Once all the symmetry directions were identified, we performed measurements of the transmission spectra, shown in Fig. 1, at several orientations of the crystal in the LU direction using a double-beam, ratio-recording UV/VIS spectrophotometer. Note that such measurements are affected by an effective absorption as a result of a diffuse scattering due to the presence of defects, dislocations, and other imperfections of the lattice. There is still another aspect of the experimental results that cannot be obviated: a small dispersion in the sphere diameter, which makes the transmission decrease steadily as the edges of the stop bands approach, instead of dropping abruptly as might have been expected from a system with a large number of planes. In order to extract the band from the transmission experimental data, we had to correctly handle all such experimental features. In the case of reflection spectra, a widely used heuristic assumption for sufficiently large crystals is to assume that the full width at half maximum (FWHM) of the reflectance peak corresponds to the bandwidth. However, when determining the band from a transmission spectrum there is no obvious criterion.

We have considered the experimental transmission at normal incidence as a function of the wavelength, shown in Fig. 2, and calculated the same transmission, shown also in Fig. 2, considering a real finite structure, that is to say, including a 2% dispersion in the sphere size, as well as an effective absorption to account for all scattering loss mechanisms present in the lattice. In the numerical calculation, all the parameters used are the actual ones, including the effective absorption coefficient, which was experimentally determined to be of the order of 15 cm^{-1}. Note that a very good match is obtained between the experimental data points and the transmission curve determined numerically using the theoretical model developed in Sect. 2. At this point, we numerically determine the transmission, using the same crystal parameters but removing the dispersion in sphere diameter and setting the effective absorption coefficient to zero. Such a transmission corresponding to the transmission of a perfect crystalline structure is also shown in Fig. 2. There are two points of intersection between the last transmission curve and the experimental transmission curve. The frequencies of these two points correspond precisely to the frequencies of the transmission resonances at the edges of the forbidden band at normal incidence. We may conclude that the width of the band, at any angle, may be obtained by setting a transmission level at 0.005, corresponding to the

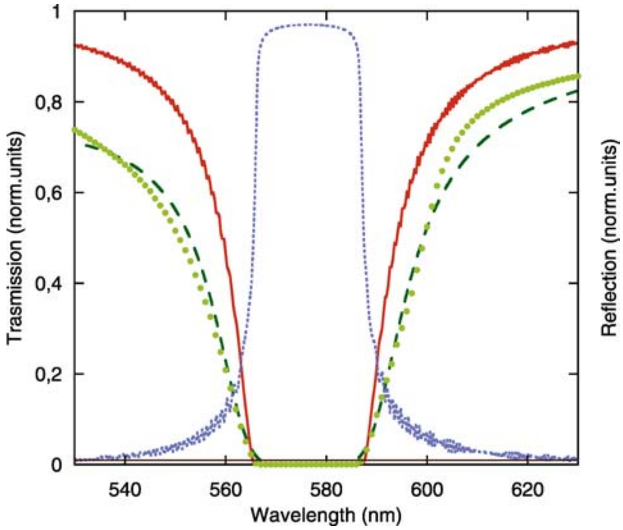

FIGURE 2 Spectral transmission of the crystal at normal incidence in the (111) direction. The *dots* correspond to the experimental measurement, the *long-dashed curve* is the calculated transmission of the crystal, the *short-dashed curve* is the calculated reflection from the same crystal, while the *solid curve* is the corresponding transmission for a perfect 200-μm-thick crystal with a lattice constant of 366 nm, without considering either dispersion in the sphere size or the presence of any defects. The *horizontal line* is the transmission level used for the band determination

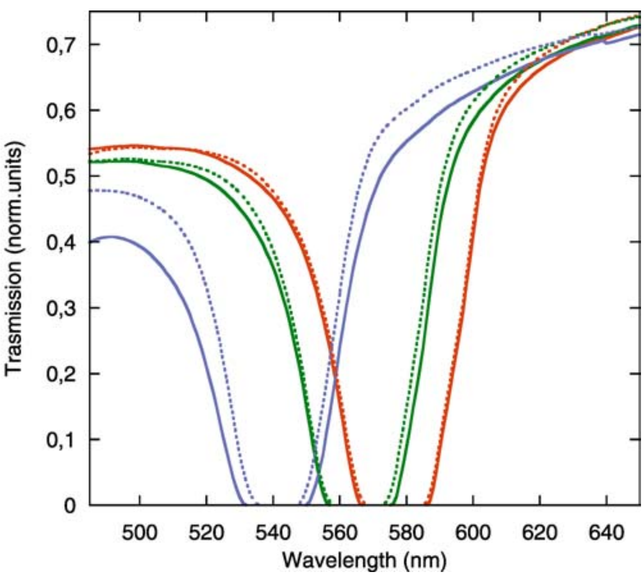

FIGURE 1 Six of the measured transmittivity spectra along the LU direction from a colloidal crystal for different angles relative to the (111) direction, expressed as a function of wavelength in vacuum. From *right* to *left*: normal incidence, 10°, 20°. The *solid* (*dotted*) curves correspond to the s polarization (p polarization) for each incidence angle

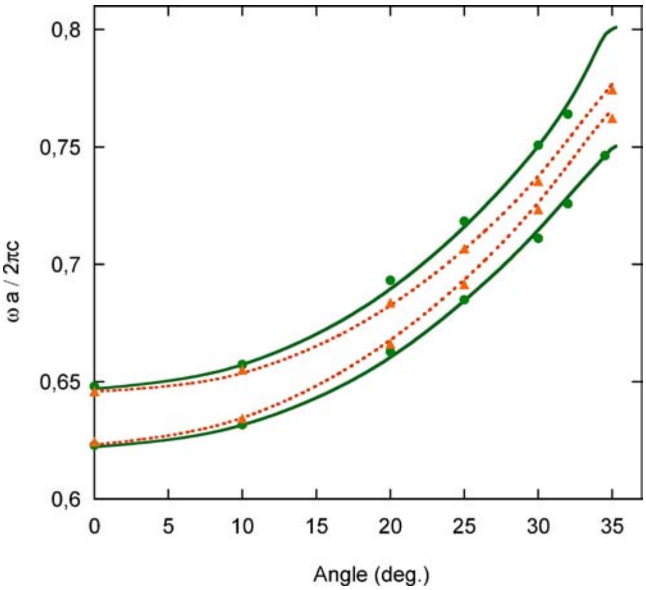

FIGURE 3 Comparison of the experimental and predicted photonic bands in the LU direction of a photonic crystal made of 920 (111) planes. *Dots* (*triangles*) correspond to the s (p) polarization measured band, while the *solid curve* (*dotted curve*) corresponds to the s (p) polarization band numerically determined using the FCM. The *vertical axis* represents frequency in reduced units $\omega a/2\pi c$

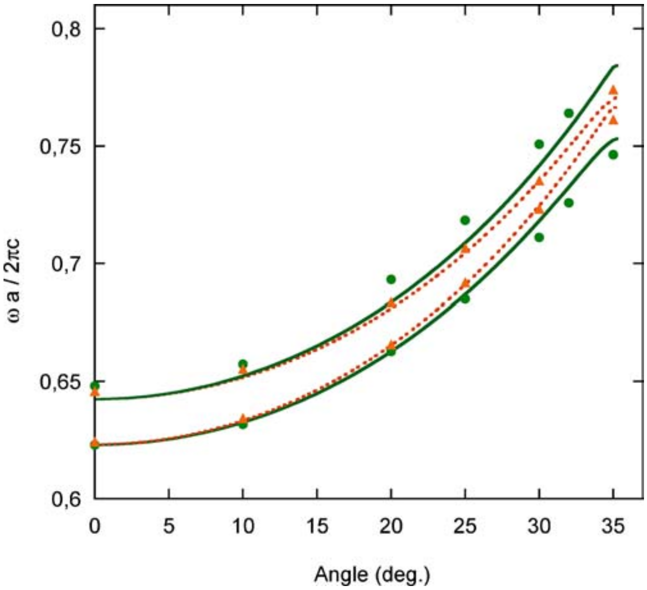

FIGURE 4 Comparison of the experimental and predicted photonic bands in the LU direction of a photonic crystal made of 920 (111) planes. *Dots* (*triangles*) correspond to the s (p) polarization measured band, while the *solid curve* (*dotted curve*) corresponds to the s (p) polarization band numerically determined using the PWM. The *vertical axis* represents frequency in reduced units $\omega a/2\pi c$

straight line shown in Fig. 2, and determining the two frequencies where such a level line intersects the corresponding experimental transmission curve. If one compares the bandwidth which results from such a procedure outlined above with the bandwidth obtained from the FWHM of a reflectivity curve, shown also in Fig. 2, one observes that both bandwidths coincide to within less than a 2.5% difference.

4 Discussion

We have applied the theoretical model developed in Sect. 2 to determine the edges of the forbidden band in the LU direction, which spans from 0° to 35.26° with respect to the normal to the (111) planes. Results from such a numerical calculation are shown in Fig. 3. All the parameters used in the numerical calculation correspond to the actual parameters of the material provided by the manufacturer of the colloidal suspension except for the surface polarization, which was determined by an experimental measurement of the transmission as a function of the angle of incidence at a fixed wavelength. A comparison between the theoretically predicted bandwidth and the one determined from the experimental measurement of the transmission[3], shown also in Fig. 3, indicates a very good agreement of the widths of the band for either the s or p polarization. There is, however, as the angle with respect to the ΓL direction increases, a slight deviation of the theoretically predicted center of the band with respect to the experimental one. Such very slight deviation of the center of the band could be attributed either to the fact that we are considering the contribution from each set of planes separately, or to the fact that we neglect the small contribution from other sets different to (111) and (200). However, such an approximation seems to have no significant effect on the width of the band.

Now, the experimentally measured LU band is compared in Fig. 4 to the band predicted by the plane wave expansion method (PWM). For this numerical determination we have adapted the method developed in Ref. [20]. In this case we observe that, although the PWM can predict the center of the band very well, the widths of the experimentally measured bands, as the angle with respect to the normal increases, is larger than the predicted ones.

To clarify the above comparisons, we have calculated the relative bandwidth deviation from the experimental data for both the above-developed finite crystal method (FCM) and PWM predictions for the s and p polarizations. Since the bandwidth at normal incidence is slightly dependent on the criterion used for the band determination, and our calculation using the PWM exhibits a slight discrepancy already at normal incidence, we have, in fact, calculated such an error relative to the bandwidth error at normal incidence. In other words, no deviation from the experimental data is assumed at normal incidence for any band, as seen in Fig. 5. Note that for the s polarization, the FCM relative error in the bandwidth is almost constant and lies below 3%, while the PWM error increases as one moves closer to the U point. In fact, at angles larger than 30° the deviation from the experimental data for the PWM case is as high as 11%. For the p polarization we observe a larger deviation for both models. However, for the FCM model, deviation at any angle is always below 10% while for the PWM such a deviation (the relative error) can be as high as 60% at the U point. Such large deviations of the PWM calculated bandwidth with respect to experimental data are not specific to colloidal crystals or to a band determination based on transmission measurements. As a matter of fact, the LU band of an opal of silica spheres determined from reflection

[3] At zero degrees one observes a slight difference between the s and p polarization experimentally measured bands. This can be most probably attributed to imperfections in the crystalline lattice.

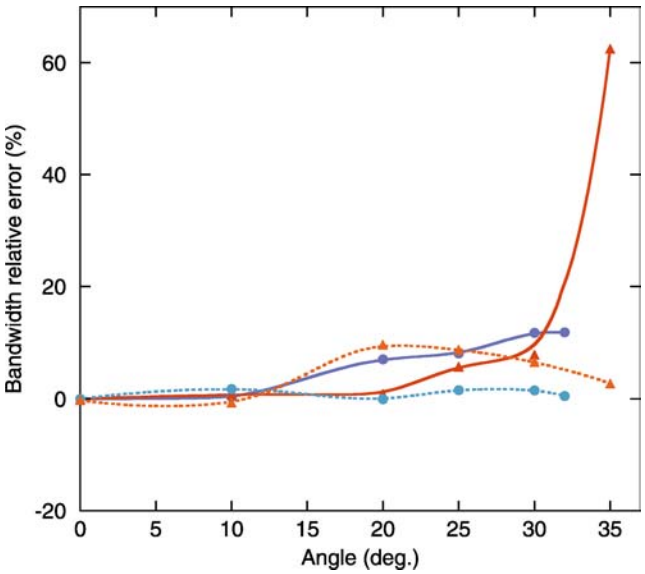

FIGURE 5 Relative deviations of the FCM (*dashed line*) and PWM (*solid line*) calculated bands with respect to the experimentally measured ones. The *circles* correspond to the s polarization band while the *triangles* correspond to the p polarization band. The *lines* are a guide for the eye

measurements was shown to exhibit a 36% discrepancy with the PWM prediction at an angle very close to the U point [8]. Note that such discrepancies exist even below an internal angle of 32° where the differences between the LU, LK, and LW bands are very small, meaning that they are present in all the lower bands of the fcc structure.

5 Conclusions

In conclusion, we have developed a three-dimensional model, which enables us to calculate the propagation of the field for both polarizations in a finite photonic crystal. We have performed an optical study of the LU band of a fcc crystal. From measurements of the transmission as a function of the wavelength of the incident light we have determined such band. We have clearly shown that while, as one moves from the L point to the U point, the PWM gives an accurate prediction of the center of the bands, it fails in determining their widths. Nevertheless, we have seen that such bandwidths, for both the s and p polarization cases, can be very accurately predicted using a theoretical model which does not impose any periodic boundary conditions in the direction perpendicular to any of the set of planes, which we use to determine such branch of the band structure. Thus, we believe that in those cases where the bandwidth plays a determining role, such as for instance when calculating the degree of inhibition of the spontaneous emission, our model could be used to obtain a better prediction than the one provided by the PWM. Moreover, the fact that no periodic boundary conditions in the direction perpendicular to the set of planes are applied in the model presented suggests that if such a finite character were to be applied to other models, one might be able to close the gap between the experimental observations and the predictions of previous band-structure calculations.

ACKNOWLEDGEMENTS We acknowledge the Ministerio de Ciencia y Tecnología, which supported the work under the program of 'Plan Nacional de Materiales' (Grant No. MAT2002-04603-C05-01). JM acknowledges support from the Generalitat de Catalunya, which awarded him in 2002 the 'Distinció de La Generalitat de Catalunya per a la Promoció de la Recerca Universitària'.

REFERENCES

1 E. Yablonovitch, Phys. Rev. Lett. **58**, 2059 (1987)
2 C.M. Soukoulis (ed.), *Photonic Crystals and Light Localization* (NATO Sci. Ser.) (Kluwer, Dordrecht, 2001)
3 B.A. van Tiggelen, S.E. Skipetrov (eds.), *Wave Scattering in Complex Media: From Theory to Application* (NATO Sci. Ser. II: Math. Phys. Chem. **107**) (Kluwer, Dordrecht, 2003)
4 K.M. Leung, Y.F. Liu, Phys. Rev. Lett. **65**, 2646 (1990)
5 Z. Zhang, S. Satpathly, Phys. Rev. Lett. **65**, 2650 (1990)
6 K.M. Ho, C.T. Chan, C.M. Soukoulis, Phys. Rev. Lett. **65**, 3152 (1990); C.T. Chan, K.M. Ho, C.M. Soukoulis, Europhys. Lett. **30**, 563 (1991)
7 I.I. Tarhan, G.H. Watson, Phys. Rev. Lett. **76**, 315 (1995)
8 J.F. Galisteo-López, F. López-Tejeira, S. Rubio, C. López, J. Sánche-Dehesa, Appl. Phys. Lett. **82**, 4068 (2003)
9 J. Martorell, N.M. Lawandy, Phys. Rev. Lett. **65**, 1877 (1990)
10 E.P. Petrov, V. Bogomolov, I. Kalosha, S. Gaponenk, Phys. Rev. Lett. **81**, 77 (1998)
11 A. Blanco, C. López, R. Mayoral, H. Míguez, F. Meseguer, A. Mifsud, J. Herrero, Appl. Phys. Lett. **73**, 1781 (1998)
12 X.-H. Wang, R. Wang, B.-Y. Gu, G.-Z. Yang, Phys. Rev. Lett. **88**, 093902 (2002)
13 D. Felbacq, R. Smaâli, Phys. Rev. B **67**, 085105 (2003)
14 J. Martorell, J. Opt. Soc. Am. B **19**, 2075 (2002)
15 C.F. Boheren, D.H. Huffman, *Absorption and Scattering of Light by Small Particles* (Wiley, New York, 1983)
16 S.H. Lou, L. Tsang, C.H. Chan, A. Ishimaru, J. Electromagn. Waves Appl. **5**, 835 (1991)
17 J.E. Sipe, J. Opt. Soc. Am. B **4**, 481 (1987)
18 N.A. Clark, A. Hurd, B.J. Ackerson, Nature **57**, 281 (1979)
19 P. Pieranski, E. Dubois-Violette, F. Rothen, L. Strzelecki, J. Phys. (Paris) **42**, 53 (1981); P. Piretanski, Contemp. Phys. **24**, 25 (1983)
20 S. Guo, Opt. Express **11**, 167 (2003)